



The Open Electrical & Electronic Engineering Journal

Content list available at: www.benthamopen.com/TOEEJ/

DOI: 10.2174/1874129001812010063, 2018, 12, 63-74



RESEARCH ARTICLE

A Study on the Design of an Outer Rotor and Spoke Type PMSM for Improving Power Density

Hak Jung Kim, Sooyoung Cho, Gang Seok Lee, Hyung-Kwan Jang, Ye Jun Oh and Ju Lee*

Department of Electrical Engineering, Hanyang University, Seoul, South Korea

Received: May 4, 2018

Revised: July 19, 2018

Accepted: July 20, 2018

Abstract:

Object:

This paper proposes an outer rotor and spoke-type permanent magnet synchronous motor (outer rotor spoke-type PMSM) to increase the power density compared to the inner rotor spoke-type permanent magnet synchronous motor (inner rotor spoke-type PMSM) used in washing machines.

Method:

In order to investigate the output characteristics of the Outer Rotor Spoke-type PMSM, comparison and analysis were conducted on three models of 16-poles/9-slots, 20-pole/9-slots and 22-poles/9-slots. Compare models were conducted with the limited condition which applies the same current density, phase voltage limit, and stator. The final model was optimized based on the model with the best output characteristics among three compare models.

Conclusion:

Finally, output characteristics are compared between compare models and the final model.

Keywords: Washing Machine, Direct Drive Motor (DD Motor), Spoke-type PMSM, Torque transmission, Electric motors.

1. INTRODUCTION

In the past, electric motors for washing machines delivered torque between the motor and the load through torque transmission mechanisms such as belts and gears. However, the electric motors for washing machines recently have been changed into a Direct Drive system (DD system) which can be driven by directly connecting a motor and a load. When a torque transmission mechanism is used, there are problems such as deterioration of washing ability, energy loss, increase of noise and belt wear due to mechanical loss occurring in the torque transmission mechanism occur [1]. On the other hand, the DD system is simple in torque transmission structure, and it is possible to achieve low noise, low vibration, and small size [2 - 4]. In addition, in case of an emergency, the brake must operate quickly. In a washing machine using a torque transmission mechanism, an indeterminate element such as a slip in a belt during a rapid brake occurred. However, the DD system does not require a complicated mechanical structure, so it can operate quickly by controlling the brake mode.

Electric motors for washing machine using a DD system mainly use a permanent magnet synchronous motor using a rare earth permanent magnet because high power density is required for a washing motor [5]. However, rare earth permanent magnet has price instability and disadvantage that it is relatively expensive compared to non-rare permanent magnets. Therefore, studies on designing motors with high power density using non-rare-earth permanent magnets are underway [6 - 10]. For example, there is Switched Reluctance Motor (SRM) [11 - 14] which rotate at a reluctance

* Address correspondence to this author at the Department of Electrical Engineering, Hanyang University, P.O. Box: 04763, Seoul, South Korea; Tel: +81-2-2220-0342; E-mails: julee@hanyang.ac.kr

torque without using a permanent magnet and Interior Permanent Magnet Synchronous Motor (IPMSM) [15, 16] which permanent magnets are radially inserted into a rotor. It has a higher power density than a permanent magnet motor with a non-magnetic flux concentrating structure like a surface permanent magnet synchronous motor (SPMSM) because it has a magnetic flux concentrating structure [2, 17 - 19].

The torque of motors increases in proportion to the number of poles [20]. Therefore, most motors can increase power density by selecting the number of poles in motor considering the switching frequency of the controller. In the inner rotor spoke-type PMSM, it is difficult to increase the number of poles structurally because the rotor is located inside the stator. On the other hand, if the rotor of the spoke-type PMSM is designed outside the stator, degree of freedom of the poles increases, so that power density of the motor can be increased.

This paper proposes an outer rotor spoke-type PMSM with higher power density than the inner rotor spoke-type PMSM used in conventional washing machines.

In Chapter 2, overall load characteristics of the base model used as a washing machine motor were analyzed. As a model of the inner rotor spoke-type PMSM, the load-speed torque curve including two operation regions of washing mode and spinning mode is presented. Also, the detailed design specifications and power density per volume of the base model are presented.

In Chapter 3, outer rotor spoke-type PMSM design with the same load demand characteristics as the base model was carried out. Three models of 16-poles / 9-slots, 20-pole / 9-slots, and 22-poles / 9-slots with different poles were proposed for compare models. Where, three compare models have the same magnetomotive force, and the magnitude of the rotor and the stator are the same. In the washing mode and spinning mode, two operation areas of the washing machine, the output characteristics of the three compare models were compared through FEM analysis and the model with the highest power density was selected.

In Chapter 4, the final model was optimized based on the model with the best output characteristics among three compare models. Through this, the final model with maximum power density while satisfying load requirements is presented.

2. SPECIFICATIONS OF EXISTING MODELS

It is necessary to analyze the load characteristics and design specifications of the motor used in the conventional washing machine. The base model motor was selected as inner rotor spoke-type PMSM with 8-poles and 12-slots as shown in Fig. (1). The selected motor for washing machine has two load characteristics as a washing mode at 580 rpm and a rotating mode at 15660 rpm. These characteristics are determined by load torque that static frictional force of the laundry while the motor is stopped and the time variation of the angular velocity. In the washing mode, relatively low speed and higher torque operation are required because it is necessary to remove some dust and detergent in the laundry. However, in the spinning mode, the high-speed low-torque operation is required for removal of moisture in the laundry.

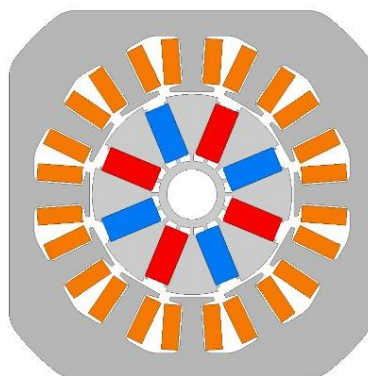


Fig. (1). Inner rotor spoke-type PMSM (Base Model).

The load demand speed torque curve is shown in Fig. (2). PMSM typically have a wide operating range through voltage controls and field weakening control. Voltage control is executed below rated speed and field weakening

control is implemented above-rated speed. The base model drives maximum torque up to 580 rpm through the voltage control which increases the impressed voltage to the rated voltage in proportional to the speed. If the impressed voltage reaches the voltage limit at the rated speed, the voltage control becomes impossible because the voltage can be no longer be increased in proportion to the speed. Therefore, the magnetic flux gradually decreases through the field weakening control and the constant power region is performed as the speed increases. The base model requires a constant torque region of 1.634 Nm at rated speed of 580 rpm through voltage control in the washing mode. In the spinning mode requiring a high-speed operation, the torque of 0.291 Nm is required at 15660 rpm by weak field weakening control.

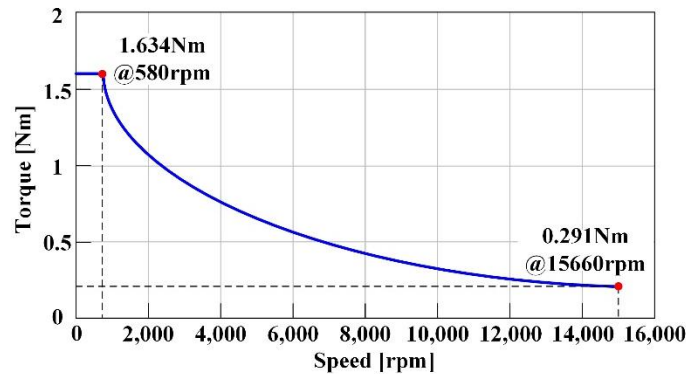


Fig. (2). Torque-Speed curve of the washing machine.

The design specifications and design data of the base model are shown in Tables 1 and 2. The power density of base model is 0.186 W/cm³ for washing mode and 0.895 W/cm³ for the spinning mode. In addition, the base model used a ferrite magnet, and the phase voltage limit is selected as 161 V considering space vector pulse width modulation (SVPWM).

Table 1. Motor design specification.

Contents	Washing	Spinning
Speed [rpm]	580	15660
Torque [Nm]	1.63	0.29
Power [W]	99.25	477.57
DC Bus Voltage [V]	310	
Rated Voltage [V]	161	
Rated Current [A _{rms}]	2.3	
Volume [cm ³]	533.47	
Power Density [W/cm ³]	0.186	0.895

Table 2. Motor design data.

Contents	Value
Number of Slots	12
Number of Poles	8
Number of Turns	90
Slot Area [mm ²]	225
Current Density [A _{rms} /mm ²]	4.59
Rotor Diameter [mm]	60
Stator Diameter [mm]	134
Air-gap width [mm]	0.75
Core length [mm]	46

Recently, research on achieving small-sizing and cost competitiveness of washing machines is continuously ongoing. The motor design that to reduce the volume while meeting the same output can reduce material cost and

achieve the goal of miniaturization and weight reduction of the product. In the next chapter, the design to increase power density with the same material as the base model was conducted.

3. DESIGN OF OUTER ROTOR SPOKE TYPE PMSM

In this chapter, three compare models are designed and analyzed by using outer rotor spoke-type PMSM to increase power density compared to the base model. Outer rotor spoke-type PMSM has more freedom to use poles than inner rotor spoke-type PMSM. Since the torque of the PMSM has a characteristic proportional to pole-pair number as shown in Equation (1), the torque can be increased as pole pairs number increases. So, compared and analyzed the output characteristics of three models with a different number of poles.

$$T = P_n \left\{ \Psi_a i_q + (L_d - L_q) i_d i_q \right\} \quad (1)$$

Where, P_n is the Pole-pair number, Ψ_a is No-load flux linkage, i_d and i_q is the current of d-axis and q-axis, L_d and L_q is the inductance of d-axis and q-axis, respectively.

The design of outer rotor spoke-type PMSM was conducted according to the number of poles of the permanent magnet. The number of poles of the permanent magnet can be selected up to 22 poles considering the switching frequency. Therefore, compare models were selected for outer rotor spoke-type PMSM with 16-poles/9-slots (Model 1), 20-pole/9-slots (Model 2), 22-poles/9-slots (Model 3), and the current density and phase voltage were fixed to be the same value.

3.1. Three Types of Compare Models

Compare models have common design specifications as shown in Table 3 to analyze the output characteristics. The ferrite magnet was used in the base model was used for the compare models. It is also analyzed in the washing and spinning mode considering the operating characteristics of the washing machine. In the washing mode, the compare models were analyzed to have the same magnetomotive force. In addition, the current density was selected to be $4.59 \text{ A}_{\text{rms}}/\text{mm}^2$ considering the slot area, the phase current, and the number of turns in order to make the current density the same as the base model.

Table 3. Common design considerations.

Contents	Value
Rotor Diameter [mm]	134
Stator Diameter [mm]	98
Magnet Material	7BE 0.38T
Iron Core Material	50PN1300
Coil	Aluminum
Air-gap width [mm]	0.75
Slot Area [mm ²]	222.22
Rated Current [A_{rms}]	5.3
Number of Turns	88
Current Density [$A_{\text{rms}}/\text{mm}^2$]	4.59

For the first model design, the 16P 9S model was selected as shown in Fig. (3). For the sensitivity analysis, detailed design variables were determined as Slot opening width of Rotor (W_{rso}), Slot opening width of Stator (W_{sso}), Teeth width of Rotor (W_{rt}), Teeth width of Stator (W_{st}), Shoes high of Stator (d_1), Shoes high of Rotor (d_2), and the values having a maximum output characteristic were derived.

Model1 has the same motor diameter as the base model and has selected a stack length of 28 mm in order to have the same power. As mentioned above, the design of Model 2 and Model 3 was used same stator shape with Model 1 to compare the power characteristics for the same magnetomotive force. First, Model 2 and Model 3 are Progressed detail design of rotor shape which can have maximum torque according to pole number. Next, stack length that can have the same power as the base model was analyzed, and obtained values of 28 mm and 17 mm, respectively.

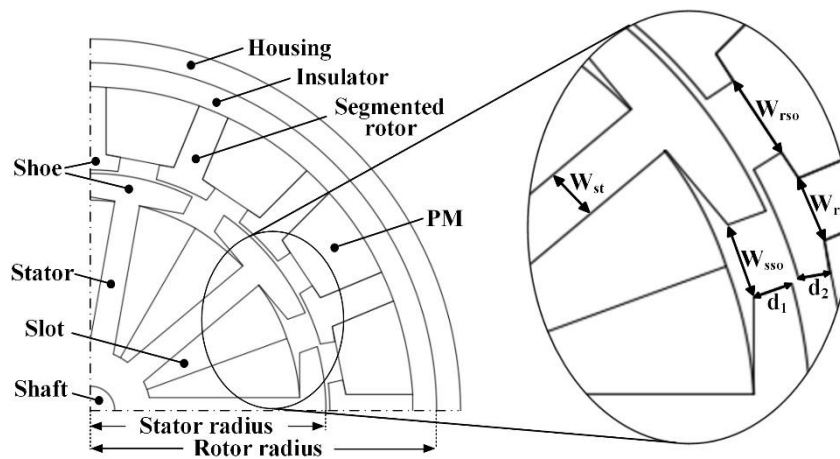


Fig. (3). Detailed design specification of Model1.

Table 4 shows the detailed design specification to have a maximum power of three compare models and shows the stack length to have the same power as the base model. Fig. (4) shows compare models based on Table 4.

Table 4. Detailed design specification.

Contents	Model1	Model2	Model3
Slot opening width of Rotor [mm]	8.2	6	4.5
Teeth width of Rotor [mm]	6.5	5.6	5.8
Shoes high of Rotor [mm]	3	2	2.5
Slot opening width of Stator [mm]	7.5		
Teeth width of Stator [mm]	5.2		
Shoes high of Stator [mm]	3.9		
Stack Length [mm]	28	28	17

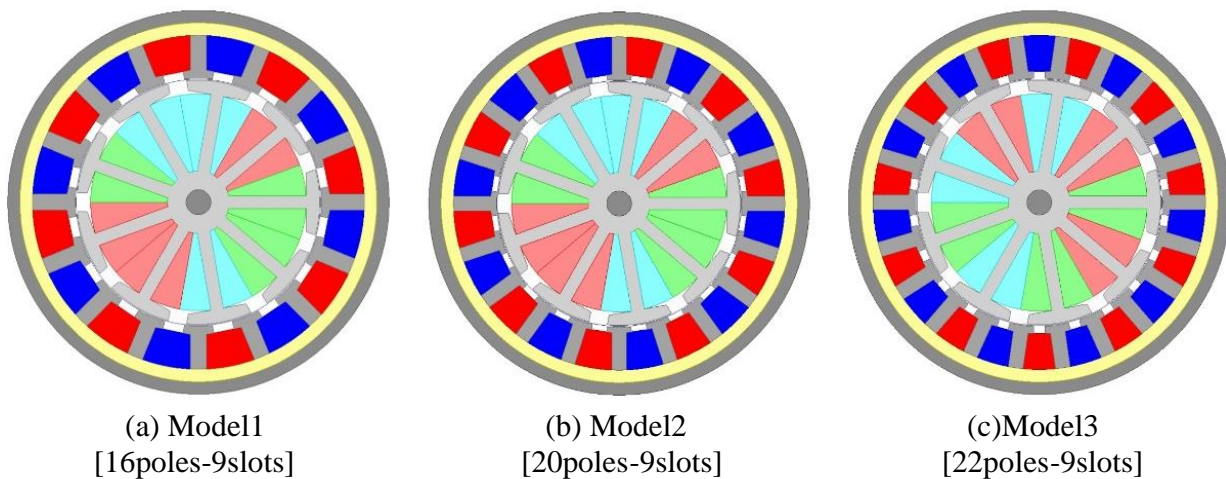


Fig. (4). Three models of outer rotor spoke-type PMSM.

3.2. Structural Characteristics of Compare Models

In the case of inner rotor spoke-type PMSM, a structure for preventing the scattering of the permanent magnet during high-speed rotation is required because of the permanent magnet inserted in the rotor. On the contrary, outer rotor spoke-type PMSM has a structure that the rotor is surrounded by the insulator and the housing as shown in Fig. (3) so that it has an advantage which is no need to design a structure to prevent scattering.

For the proposed outer rotor spoke-type PMSM, an insulator is essential. Fig. (5a) shows the results obtained by converting the insulator part into an iron core material. If the insulator is replaced by a yoke as shown in the Fig. (5a), the magnetic flux concentrates at the yoke portion having a higher magnetic permeability than the air gap. It becomes impossible to concentrate the magnetic flux into the air gap and a large amount of leakage magnetic flux is generated along the yoke. Fig. (5b) is the result of the analysis considering the insulator as shown in this paper. Since the thickness of the insulator is thicker than the thickness of air gap, the magnetic flux passes through the air gap having a small magnetic reluctance. This means that an insulator having a relatively large magnetic reluctance can have a high torque by limiting the flow of magnetic flux to be directed to the outside and directing the concentrated magnetic flux towards the air gap. Therefore, in the case of the outer rotor spoke-type PMSM, the insulator must be included in the housing and the analysis must be performed in consideration of the insulator. In this paper, 5[mm insulator and 5 mm housing were designed, and the precise analysis was performed considering the leakage flux that can occur in the housing.

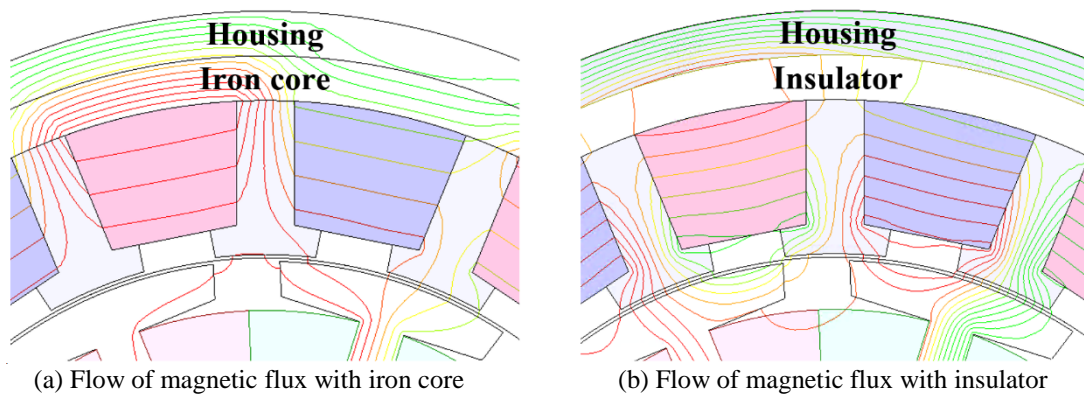


Fig. (5). Flow of magnetic flux with insulator and iron core.

3.3. Performance Comparison and Analysis

In order to confirm the power density of compare models, the design was conducted to satisfy the load demand output characteristics by adjusting the Stack Length (L_{stk}) with the same motor diameter. Figs. (6 and 7) show the torque waveforms of base model and compare models in the washing and spinning mode based on the FEM analysis. The dotted line in black indicates torque waveform of the base model, and the solid line shows the torque waveforms in the compare models.

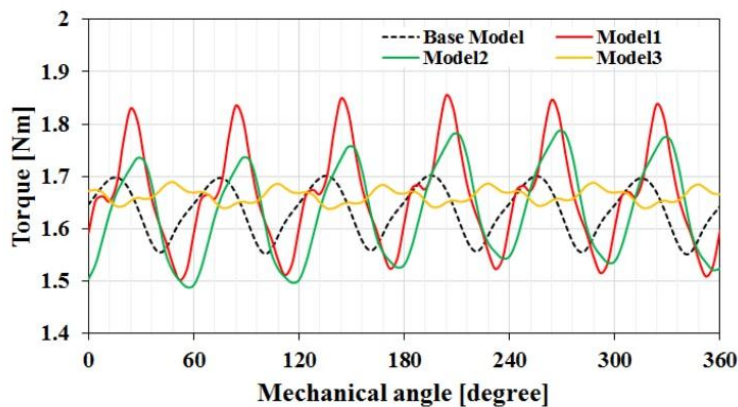


Fig. (6). Torque characteristic at washing mode.

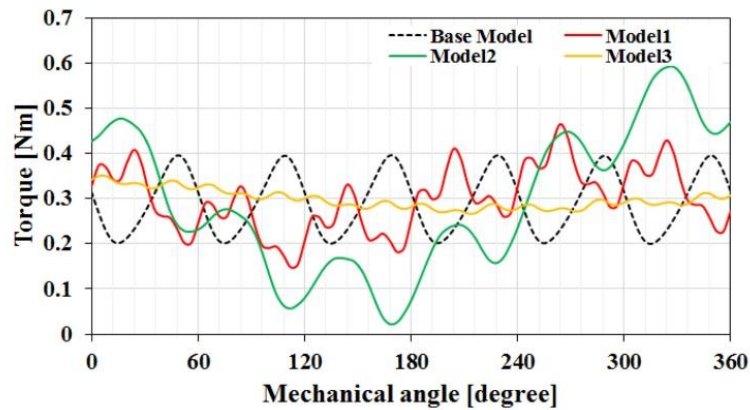


Fig. (7). Torque characteristic at spinning mode.

Table 5 shows the magnetic flux density saturation in the core by d-axis alignment of the compare models. Model1 shows proper magnetic flux saturation below 1.8 T in both operating modes. However, Model 2 and Model 3 can be seen that the stator and the rotor are partially saturated during the washing mode. The assumption can be made that the stator shape for Model1 is suitable under the same condition of the stator but for the rotor to generate more magnetic flux than Model1.

Table 5. Magnetic flux density maps at washing mode and spinning mode.

	Model1	Model2	Model3	Magnetic flux density
Washing Mode				B [tesla] 1.8000E+000 1.6800E+000 1.5600E+000 1.4400E+000 1.3200E+000 1.2000E+000 1.0800E+000 9.6000E-001 8.4000E-001 7.2000E-001 6.0000E-001 4.8000E-001 3.6000E-001 2.4000E-001 1.2000E-001 0.0000E+000
Spinning Mode				

Fig. (8) schematically shows 3D designs of the base model and the compare models. The stack lengths of the compare models are 28 mm for Model 1 and Model 2, and 17 mm for Model 3. This means that as the number of poles increases, it becomes possible to design a motor with higher air gap flux density. The detailed results of the FEM analysis are shown in Table 6. The calculation of CMPD / BMPD shows the increase rate of how much the power density of compare models (CMPD) is increased compared to the power density of the base model (BMPD). Model1 and Mode2 show 137% increase compared to Base Model and Model3 increase about 226%. Also, in the case of torque ripple, it is confirmed that in the washing mode, it becomes bigger in order of Model 1, Model 2, Base Model 1, Model 3. And it is confirmed that in the spinning mode, it becomes bigger in order of Model 2, Model 1, Base Model, Model 3. Especially, the torque ripple ratio of Model 3 was significantly reduced compared to the base model.

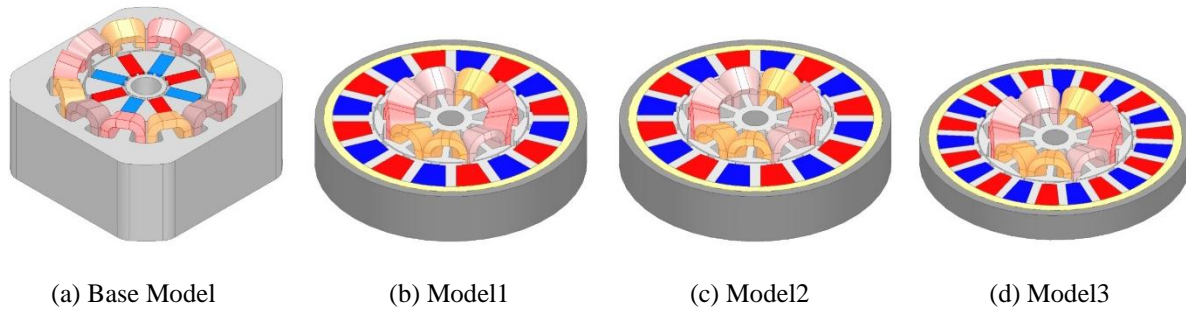


Fig. (8). 3D models of base model and compare models.

Table 6. FEM analysis results of the Base Model and compare models.

Contents	Base Model		Model 1		Model 2		Model 3	
	Washing	Spinning	Washing	Spinning	Washing	Spinning	Washing	Spinning
Phase current [A_{rms}]	2.3	2.3	5.3	3.3	5.3	3.9	5.3	2.8
Current Density [A_{rms}/mm^2]	4.9							
Current phase angle [deg]	7	80	13	63	6	64	0	63
Stack Length [mm]	46		28		28		17	
Average torque [Nm]	1.634	0.291	1.665	0.298	1.662	0.291	1.663	0.297
Torque ripple ratio [%]	9.32	67.32	21.26	106.05	18.27	193.37	3.06	27.96
Power Density [W/cm^3]	0.186	0.895	0.256	1.240	0.256	1.206	0.421	2.032
(C.M.P _D - B.M.P _D) / B.M.P _D [%]	100	100	137.63	138.55	137.63	134.75	226.34	227.04

(a) Base Model (b) Model1 (c) Model2 (d) Model3

4. FINAL MODEL

This chapter deals with the design to improve the output characteristics for Model 3 as specified in Chapter 3. Model3 reduced the diameter of the stator from 98 mm to 95 mm to increase the magnetic loading. The optimum design was performed to increase the teeth width of the rotor and reduce the teeth width of the stator through sensitivity analysis about detailed design specifications. Fig. (9) shows the shape of Model3 and final model, and Table 7 shows detailed design specifications of the final model.

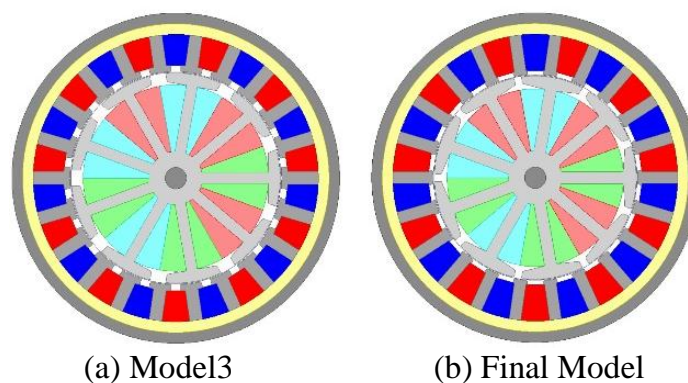


Fig. (9). Shape of Model3 and Final Model.

Table 7. Detailed design specification of Final Model.

Contents	Model 3	Final Model
Rotor Diameter [mm]	134	
Stator Diameter [mm]	98	95
Air-gap width [mm]	0.75	
Slot Area [mm ²]	444.44	388.9

(Table 9) contd.....

Contents	Model 3	Final Model
Slot opening width of Rotor [mm]	4.5	7.5
Slot opening width of Stator [mm]	7.5	3.5
Teeth width of Rotor [mm]	5.8	5.4
Teeth width of Stator [mm]	5.2	5.7
Shoes high of Stator [mm]	3.9	3.3
Shoes high of Rotor [mm]	2.5	1.8

At rated speed, Model 3 was able to show that partial saturation occurred at the stator teeth. To improve this, the teeth width of the stator was increased from 5.2 mm to 5.7 mm. Also, the shape of the rotor and shoes of the stator were optimized to solve the magnetic flux saturation. Fig. (10) shows the degree of the magnetic flux saturation of the final model and shows the stable magnetic flux density values of magnetic flux density in the rotor and stator.

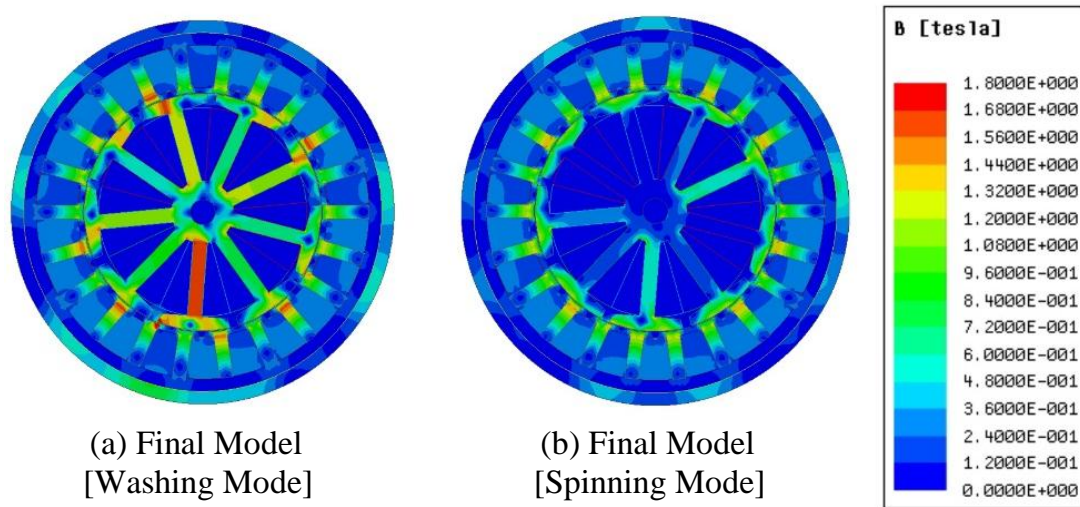


Fig. (10). Magnetic flux density maps of Final Model at washing and spinning mode.

Fig. (11) shows the torque waveform of base model and final model at washing mode 580 rpm and Fig. (12) shows the torque waveform at spinning mode 15660 rpm. The final model satisfied the average torque values of the base model in both modes. The torque ripple ratio of the final model is about 2.6% in the washing mode and about 9.7% in the spinning mode. So, its performance is much higher than the base model.

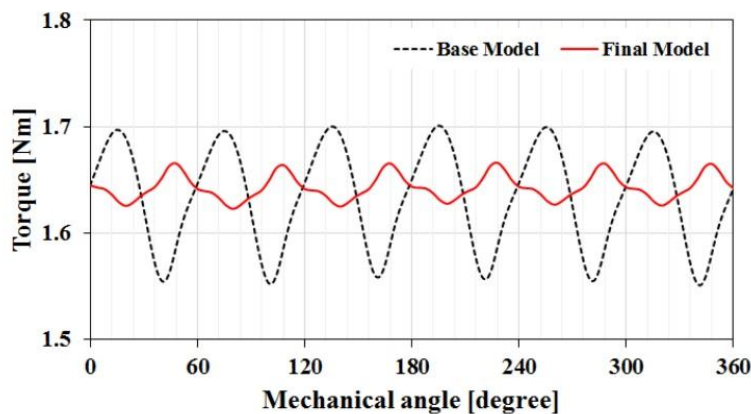


Fig. (11). Torque Characteristic of the Final Model.

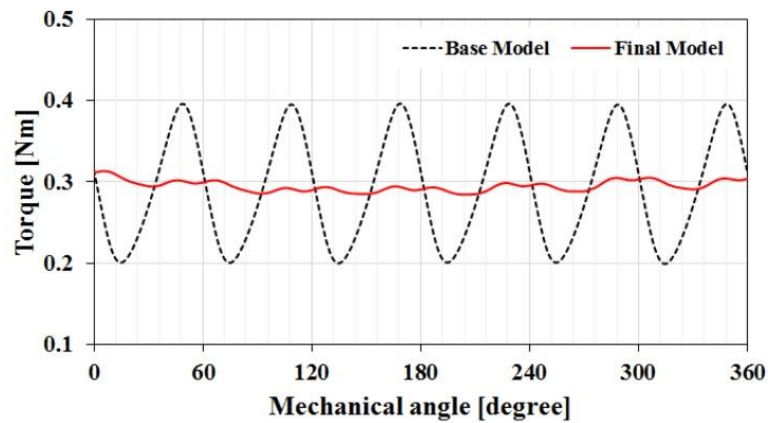


Fig. (12). Torque Characteristic of the Final Model.

The final model has the same output as the base model at the while the volume is greatly reduced to 211.54 cm³, making it possible to design as shown in Fig. (13). This effectiveness increases power density by 154% when the washing machine motor is designed by outer rotor spoke-type PMSM. Table 8 shows the detailed FEM analysis results of the final model.

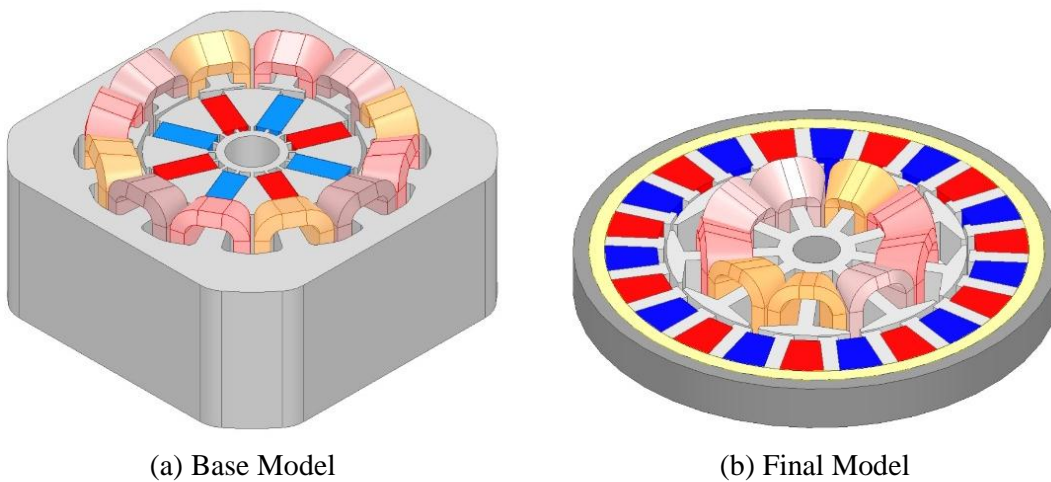


Fig. (13). 3D models of Base Model and Final Model

Table 8. FEM analysis results of the Final Model.

Contents	Base Model		Final Model	
	Washing	Spinning	Washing	Spinning
Phase current [A_{rms}]	2.3	2.3	5.2	2.8
Current Density [A_{rms}/mm^2]	4.59			
Current phase angle [deg]	7	80	4	59
Current Density [A_{rms}/mm^2]	4.59		4.59	
Stack Length [mm]	46		15	
Average torque [Nm]	1.63	0.29	1.64	0.29
Torque ripple [%]	9.32	67.32	2.63	9.70
Power [W]	99.25	477.57	99.79	483.53
Volume [cm ³]	533.47		211.54	
Power Density [W/cm ³]	0.186	0.895	0.472	2.286
(F.M.P _D - B.M.P _D)/ B.M.P _D [%]	100	100	253.76	255.42

CONCLUSION

In this paper, an outer rotor spoke-type PMSM was proposed to design a DD motor with high power density compared to the inner rotor spoke-type PMSM used as a washing machine motor. Three compare models of Model1(16-poles/9-slots), Model2(20-poles/9-slots) and Model 3(22-poles/9-slots) were designed with the same number of slots and different combinations of poles. Among the three comparative models, Model3 had the highest output density characteristics. However, Model 3 showed considerable flux saturation at the stator teeth due to the conditions of using the same stator. So, the flux saturation problem is solved by increasing the stator tooth width, and the final model which can have the maximum power density through the sensitivity analysis of a detailed design specification is derived. As a result, the final model was able to design an outer rotor spoke-type PMSM with power density increase of more than 250% compared to the base model. In addition, the torque ripple ratio of the final model has 2.63% and 9.7% in the washing mode dehydration mode, respectively. Based on the above results, it is considered that the use of outer rotor spoke-type PMSM in the field of home electric appliances and DD motors requiring high torque will be a useful method for lightening the product.

CONSENT FOR PUBLICATION

Not applicable.

CONFLICT OF INTEREST

This work was supported in part by the Korea Institute of Energy Technology Evaluation and Planning(KETEP) and the Ministry of Trade, Industry & Energy(MOTIE) of the Republic of Korea (No. 20172010105270) and in part by the National Research Foundation of Korea (NRF) grant funded by the Korea government (MSIP) (No. 2016R1A2A1A05005392).

ACKNOWLEDGEMENTS

Declared none.

REFERENCES

- [1] D-S. Jung, "The Study on the improvement of characteristics of permanent magnet synchronous motor for washing machine", *J Korean Institute Illuminat Electric Installation Engineers*, vol. 29, no. 10, pp. 47-53, 2015. [<http://dx.doi.org/10.5207/JIEIE.2015.29.10.047>]
- [2] H. Zhang, H. Xu, C. Fang, and C. Xiong, "Design of a novel speed controller for direct-drive permanent magnet synchronous motor based on reduced-order load torque observer", *ITEC Asia-Pacific*, 2017. [<http://dx.doi.org/10.1109/ITEC-AP.2017.8080864>]
- [3] K. Harmer, P. Mellor, and D. Howe, "An energy efficient brushless drive system for a domestic washing machine", *Power Electronics and Variable-Speed Drives*, 2002. [<http://dx.doi.org/10.1049/cp:19941018>]
- [4] H-J. Ahn, and D-M. Lee, "A new bumpless rotor-flux position estimation scheme for vector-controlled washing machine", *IEEE Trans. Ind. Inform.*, vol. 12, no. 2, pp. 466-473, Ari. 2016. [<http://dx.doi.org/10.1109/TII.2016.2516974>]
- [5] S.G. Lee, and W-H. Kim, "A study on the axial leakage magnetic flux in a spoke type permanent magnet synchronous motor", *Elect. Machin. Driv. Conf (IEMDC)*, 2017 [<http://dx.doi.org/10.1109/IEMDC.2017.8002126>]
- [6] S. Eriksson, and H. Bernhoff, "Rotor design for pm generators reflecting the unstable neodymium price", in *Proc. 20th ICEM*, pp. 1419-1423. [<http://dx.doi.org/10.1109/ICEIMach.2012.6350064>]
- [7] I.-M Seo, H.-K Kim, and J. Hur, "Design and analysis of modified spoke type bldc motor using a ferrite permanent-magnet", *Elect. Machin. Sys. (ICEMS)*, 2014. [<http://dx.doi.org/10.1109/ICEMS.2014.7013753>]
- [8] J. Zhu, K. W. E. Cheng, and X. Xue, "Comparison study of rare-earth-free motors with permanent magnet motors in EV applications", *Power Transfer Security (PESA)*, 2016. [<http://dx.doi.org/10.1109/PESA.2017.8277735>]
- [9] W. Wang, M. Wang, S. Zhang, P. Zheng, Z. Fu, and Y. Fang, "Electromagnetic and mechanical analyses of less-rare-earth interior permanent-magnet synchronous machine used for electric vehicles", *ITEC Asia-Pacific*, 2017. [<http://dx.doi.org/10.1109/ITEC-AP.2017.8080986>]
- [10] S. Y. Cho, H. W. Ahn, S. H. Ham, C. S. Jin, and J. Lee, "Design of fan-shape type pmsm for improving efficiency of non-rare earth motor",

- Transact Korean Instit Electric Engin.*, vol. 65, no. 2, pp. 360-364, 2016.
[<http://dx.doi.org/10.5370/KIEE.2016.65.2.360>]
- [11] A. Chiba, Y. Takano, M. Takeno, T. Imakawa, N. Hoshi, M. Takemoto, and S. Ogasawara, "Torque density and efficiency improvements of a switched reluctance motor without rare-earth material for hybrid vehicles", *IEEE Ind. Appl.*, vol. 47, no. 3, pp. 1240-1246, 2011.
[<http://dx.doi.org/10.1109/TIA.2011.2125770>]
- [12] S. Wang, Q. Zhan, Z. Ma, and L. Zhou, "Implementation of a 50-kw fourphase switched reluctance motor drive system for hybrid electric vehicle", *IEEE Trans. Magn.*, vol. 41, no. 1, pp. 501-504, 2005.
[<http://dx.doi.org/10.1109/TMAG.2004.838985>]
- [13] K.M. Rahman, and S.E. Schulz, "Design of high-efficiency and hightorque-density switched reluctance motor for vehicle propulsion", *IEEE Trans. Ind. Appl.*, vol. 38, no. 6, pp. 1500-1507, 2002.
[<http://dx.doi.org/10.1109/TIA.2002.805571>]
- [14] N. Schofield, S.A. Long, D. Howe, and M. McClelland, "Design of a switched reluctance machine for extended speed operation", *IEEE Trans. Ind. Appl.*, vol. 45, no. 1, pp. 116-122, 2009.
[<http://dx.doi.org/10.1109/TIA.2008.2009506>]
- [15] X. Ge, "A spoke-type ipm machine with novel alternate airspace barriers and reduction of unipolar leakage flux by step-staggered rotor", *IEEE Trans.*, vol. 52, no. 6, pp. 4789-4789, 2016.
[<http://dx.doi.org/10.1109/TIA.2016.2600649>]
- [16] S. Cho, H. Ahn, H. Liu, H. Hong, and J. Lee, "Analysis of inductance according to the applied current in spoke-type pmsm and suggestion of driving mode", *IEEE Trans. Magn.*, vol. 53, no. 6, 2017.
[<http://dx.doi.org/10.1109/TMAG.2017.2662719>]
- [17] W-H. Kim, I-S. Jang, C-S. Jin, and J. Lee, "Design of novel overhang structure for separated pole-piece type ferrite magnet motor", *J. Magn.*, vol. 51, no. 3, 2015.
[<http://dx.doi.org/10.1109/TMAG.2014.2346081>]
- [18] M.R. Mohammad, K-T. Kim, and J. Hur, "Design and analysis of a spoke type motor with segmented pushing permanent magnet for concentrating air-gap flux density", *IEEE Trans. Magn.*, vol. 49, no. 5, pp. 2397-2400, 2013.
[<http://dx.doi.org/10.1109/TMAG.2013.2240664>]
- [19] S. Cho, G. Jeong, J.S. Lim, Y.J. Oh, S-H. Ham, and J. Lee, "Characteristics analysis of novel outer rotor fan-type pmsm for increasing power density", *J. Magn.*, vol. 23, no. 2, pp. 247-252, 2018.
[<http://dx.doi.org/10.4283/JMAG.2018.23.2.247>]
- [20] C.-H ZHAO, H. QIN, Y.-G YAN, "Analysis of the pole numbers on flux and power density of ipm synchronous machine," *Power Electron Drives Syst*, 2006.
[<http://dx.doi.org/10.1109/PEDS.2005.1619908>]

© 2018 Kim et al.

This is an open access article distributed under the terms of the Creative Commons Attribution 4.0 International Public License (CC-BY 4.0), a copy of which is available at: <https://creativecommons.org/licenses/by/4.0/legalcode>. This license permits unrestricted use, distribution, and reproduction in any medium, provided the original author and source are credited.